



Cite this: *Photochem. Photobiol. Sci.*, 2015, **14**, 1190

## Photocatalytic water disinfection by simple and low-cost monolithic and heterojunction ceramic wafers†

Neel M. Makwana, Rachael Hazael, Paul F. McMillan and Jawwad A. Darr\*

In this work, the photocatalytic disinfection of *Escherichia coli* (*E. coli*) using dual layer ceramic wafers, prepared by a simple and low-cost technique, was investigated. Heterojunction wafers were prepared by pressing TiO<sub>2</sub> and WO<sub>3</sub> powders together into 2 layers within a single, self-supported monolith. Data modelling showed that the heterojunction wafers were able to sustain the formation of charged species (after an initial "charging" period). In comparison, a wafer made from pure TiO<sub>2</sub> showed a less desirable bacterial inactivation profile in that the rate decreased with time (after being faster initially). The more favourable kinetics of the dual layer system was due to superior electron–hole vectorial charge separation and an accumulation of charges beyond the initial illumination period. The results demonstrate the potential for developing simplified photocatalytic devices for rapid water disinfection.

Received 2nd January 2015,  
Accepted 5th May 2015

DOI: 10.1039/c5pp00002e

www.rsc.org/ppps

In 2012, the United Nations estimated that nearly 11% of the world's population did not have access to improved sources of drinking water, with *ca.* 3.5 million deaths annually attributed to unsafe water supplies, poor sanitation and unsatisfactory hygiene.<sup>1</sup> With ever-increasing populations, there is now an unprecedented demand to improve basic water facilities, particularly in rural regions of less economically developed countries. The ideal solution would be to improve sanitation infrastructure, however, this is often associated with large cost and may not be practical to implement quickly. Short-term solutions that provide clean drinking water at the point-of-use are regularly used, such as boiling and filtration techniques. However, these are not effective at removing all pathogens. Over the last decade, solar disinfection techniques such as SODIS (Solar DISinfection) have been developed and used by over a million people.<sup>2–4</sup> SODIS typically involves filling a glass or plastic bottle with contaminated water and placing the bottle in direct sunlight (*e.g.* on a roof) for at least 6 hours, which exposes pathogens to UVA radiation and thus, inactivates them. After this exposure, the water is deemed safe to drink. However, while the SODIS technique is simple and easy to implement, it has limitations that can lead to the drinking water being unsafe. Main limitations concern the type of

bottle used (a maximum volume of 3 litres), the turbidity of the water (*i.e.*, placing the bottle on a newspaper should allow the headline text to be read through the bottled water), and the shelf-life of the SODIS-cleaned water that should be consumed within 24 hours.<sup>2</sup> Based on these considerations, the SODIS technique can only be used as a point-of-use intervention, rather than for large-scale water disinfection. Thus, there is a real need to develop simple and inexpensive alternatives to SODIS that are able to provide larger volumes of clean drinking water.

An alternative approach to SODIS is to use semiconductor photocatalysts to efficiently achieve solar water disinfection without the limitations of SODIS. In this approach, the semiconductor photocatalyst undergoes a series of photoelectrochemical processes that result in the formation of reactive species that are able to more rapidly inactivate pathogens. In the first step, illumination of the semiconductor by light of an appropriate wavelength can excite electrons from the valence to the conduction band, leading to the formation of an electron–hole pair. The charge carriers can then either recombine (with no catalytic reaction) or they can migrate to the semiconductor surface where they can participate in surface reactions to form radicals, typically reactive oxygen species (ROS). These radical species are powerful redox agents that can rapidly destroy organic pollutants and inactivate many pathogens.

Amongst the range of semiconductor photocatalysts available for disinfection, titanium dioxide (TiO<sub>2</sub>) has received most interest, as it is inexpensive, relatively abundant, stable, non-toxic and photoactive under UV light illumination.

Christopher Ingold Laboratories, Department of Chemistry, University College London, 20 Gordon Street, London, WC1H 0AJ, UK. E-mail: j.a.darr@ucl.ac.uk  
† Electronic supplementary information (ESI) available: Band energy diagram of type II heterostructure, X-ray diffraction pattern, scanning electron microscopy images and xenon lamp spectral output. See DOI: 10.1039/c5pp00002e



However, there are still many challenges that limit the use of TiO<sub>2</sub> in large-scale applications, *e.g.* its wide band-gap (3.2 eV) means it is excited by UV (or higher energy) radiation, which only makes up *ca.* 4% of the total solar light incident on Earth. Efforts have been made to increase the absorption of light by TiO<sub>2</sub>, *e.g.* by incorporating dopant species that narrow the band-gap.

The need to reduce recombination reactions is also important in solar applications. Charge carriers in TiO<sub>2</sub> can recombine within nanoseconds,<sup>5</sup> and if surface reactions occur on longer timescales then recombination processes can reduce activity. One approach used to improve efficiencies in photocatalysis is to couple two or more appropriate photoactive materials into heterojunction thin films (directly from vapour deposition) or as monoliths (from powders).<sup>6–12</sup> When appropriate semiconductors are chosen, the band alignment is such that the positions of the conduction band (CB) and valence band (VB) of one semiconductor are higher than that of the other semiconductor (type II staggered bandgap heterostructure; see Fig. S1†).<sup>13</sup> Under photoirradiation, electrons can transfer across the heterojunction from one semiconductor to the other, *i.e.* from the higher CB level to the lower CB level. Conversely, holes can transfer from the lower VB level to the higher VB level.<sup>12,14</sup> Consequently, photogenerated electrons and holes migrate to different sides of the device where they are trapped, thereby removing or reducing electron–hole recombination. The vectorially charge separated electrons and holes are then able to participate in specific chemical reactions at the respective photoelectrochemically activated surfaces.

Typically, photocatalytic disinfection experiments are conducted with either the photocatalyst suspended in solution or immobilised on a substrate. Although placing the photocatalyst in suspension can yield high efficiencies,<sup>15</sup> it is often difficult to recover the photocatalyst,<sup>16</sup> and therefore photocatalysts immobilised on surfaces are of interest.<sup>17–25</sup>

The authors recently described a simple method for producing robust, self-supported ceramic wafers of TiO<sub>2</sub>, formed by cold-pressing commercially available powders.<sup>26</sup> The technique has now been used to prepare self-supported photocatalytic bilayer heterojunction (SPH) wafers from powdered TiO<sub>2</sub> and WO<sub>3</sub>.<sup>27</sup> Upon illumination of SPHs, electron transfer from TiO<sub>2</sub> to WO<sub>3</sub> occurred, resulting in the formation of reduced tungsten oxidation states. Despite the simplicity of the fabrication process for the SPH, intimate electronic contact between the two layers was achieved. Consequently, the SPH wafers showed enhanced photocatalytic performance compared to comparable individual photocatalyst wafers for photocatalytic destruction of stearic acid (a model pollutant).<sup>28</sup> Herein, we compare the photocatalytic action between a heterojunction-type wafer (TiO<sub>2</sub>–WO<sub>3</sub>) and a non-heterojunction wafer (pure TiO<sub>2</sub>) for disinfection of water, by photoirradiating wafers placed in a saline solution contaminated with the Gram-negative bacterial pathogen *E. coli* K-12, (a widespread infective agent found in water). Photodisinfection using the dual layer SPH wafer was highly effective and superior to the wafer of pure TiO<sub>2</sub>.

## Experimental methods

### Bacterial cultivation

All experiments were conducted with *Escherichia coli* (*E. coli*) K-12 (DSM 5210) obtained from the Deutsche Sammlung von Mikroorganismen und Zellkulturen GmbH, DSMZ (Braunschweig, Germany). Following rehydration of the bacterial strain, a single colony was taken and subcultured in 10 mL Lysogeny broth (LB) at 37 °C for 18 hours under an agitation of 250 rpm. Cells were harvested in a stationary phase to obtain *ca.* 10<sup>6</sup> CFU per mL (colony forming units per mL); 1 mL of this suspension was removed and centrifuged at 3000 rpm for 10 min, and the supernatant was discarded before re-suspending the bacteria in 1 mL 0.9% NaCl solution (sterile). The centrifugation was repeated twice, with the supernatant replaced with fresh NaCl solution each time.

### Preparation of TiO<sub>2</sub> and TiO<sub>2</sub>–WO<sub>3</sub> ceramic wafers

TiO<sub>2</sub> ceramic wafers were prepared by pressing TiO<sub>2</sub> powder (anatase PC50; Cristal Global, Stallingborough, UK) in a circular 25 mm diameter stainless steel die (Compacting Tooling Inc., Philadelphia, USA). The TiO<sub>2</sub> powder (0.3 g) was placed in the die and levelled to create an even surface. The powder was pressed at a pressure of 200 bar in the extraction ram of a non-end-loaded piston cylinder device (Depths of the Earth Co., Arizona, USA).<sup>29</sup> To prepare the layered TiO<sub>2</sub>–WO<sub>3</sub> ceramic wafers, TiO<sub>2</sub> powder (0.3 g) was placed in the die and levelled to create an even surface, followed by addition of WO<sub>3</sub> powder (99.8% metals basis; Alfa Aesar, Lancashire, UK; 0.7 g), and the layers were then pressed following the procedure described above. The ceramic wafers were heat-treated at 500 °C for 6 h in air to enhance their mechanical strength. Material characterization data (X-ray diffraction pattern and scanning electron microscopy images) are provided in Fig. S2 and S3 in the ESI.†

### Disinfection experiments

Each experiment was conducted in 60 mL 0.9% NaCl solution (prepared using deionised water; >15 MΩ resistivity) with UV-visible light photoirradiation provided by a 75 W Xe arc lamp (Photon Technology International, UK) with an AM 1.5 G filter (Newport Spectra-Physics Ltd, UK; spectral output shown in Fig. S4†) to simulate solar irradiation. Where used, an inoculum of 60 μL *E. coli* suspension in NaCl (0.9%) was added to achieve an initial cell density of 10<sup>6</sup> CFU per mL. To avoid any thermal effects arising from the Xe lamp, all experiments were conducted in a double-walled glass reactor with cooling water (20 °C) circulated through the outer wall (ThermoHake 75 chiller). During the experiments, samples of the test solution (0.5 mL) were collected from the photoreactor at regular intervals. For bacterial enumeration studies, each recovered sample was subjected to a series of 10-fold dilutions in 0.9% NaCl solution, followed by triplicate plating and each plate was incubated at 37 °C for 15 hours. Standard methods were used to visually identify and count colonies. Control experiments were carried out in the dark to determine any potential effects from the saline solution and photocatalyst on the *E. coli* sample in



the absence of photoexcitation and to ensure that no external factors contributed to cell death.

### Data fitting models

The *E. coli* survivability data were fitted using the Geeraerd and Van Impe Inactivation Model Fitting Tool (GInaFiT, v1.6).<sup>30</sup> A number of fitting models were run for each data set; comparison between the fit of each model was possible by assessing the value of the Root Mean Sum of Squared Errors (RMSE). The RMSE is considered the most simple and informative measure of goodness-of-fit, where a smaller value indicates a better data fit.<sup>31</sup> For the data presented herein, it was found that the 'log-linear with shoulder', 'Weibull' and 'Weibull with tail' models<sup>32,33</sup> were most appropriate for the SODIS, TiO<sub>2</sub> and SPH wafers, respectively. The output fitting curves are shown along with the bacterial survival data.

## Results and discussion

A series of initial controls were conducted to calibrate for any potential effects of the experimental conditions on *E. coli* in saline solution. Such effects included osmotic and mechanical stresses (imposed by the saline solution and stirring), temperature, pH, and the nature of the surrounding environment, in the absence of light. We observed no significant decrease in bacterial survivability under these experimental conditions; this observation also held true when testing with the photocatalytic wafers suspended in the solution in the dark (Fig. 1). However, when the reactor was illuminated without a pressed wafer present, a decrease in bacterial survivability did occur after ca. 2 hours of irradiation, demonstrating that the UV light partially and directly inactivated *E. coli*. Similar results have been reported previously using simulated or real solar conditions, with slow *E. coli* inactivation observed in the range

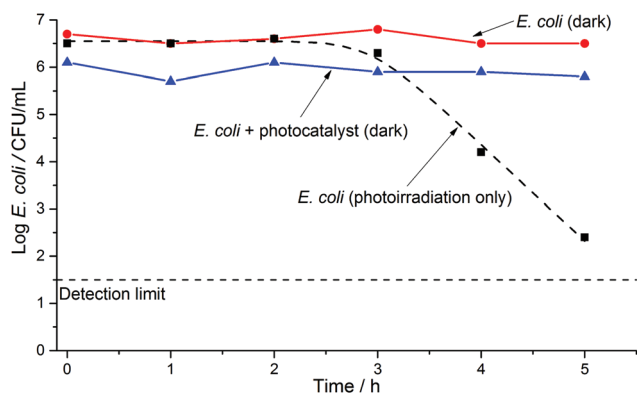


**Fig. 1** *E. coli* inactivation control experiments over a 5 hour period; filled circles (●) show inactivation of *E. coli* in solution in the dark; filled triangles (▲) show inactivation in the presence of a TiO<sub>2</sub>-WO<sub>3</sub> wafer in the dark; filled squares (■) show inactivation under irradiation from a 75 W xenon lamp (in the absence of the wafer); simulated solar disinfection, SODIS. The dashed line [---] shows a data fit using the log-linear with shoulder model.

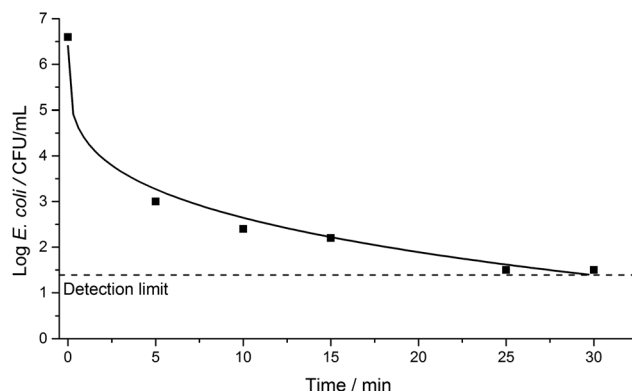


**Fig. 2** *E. coli* inactivation over a 30-minute period under irradiation from a 75 W xenon lamp in the presence of a TiO<sub>2</sub> ceramic wafer. The solid line shows a data fit using the Weibull model.

ca. 2 to 6 hours.<sup>3,4,23,34–37</sup> These observations are in line with expectations and demonstrate SODIS water disinfection.

Fig. 2 shows the *E. coli* inactivation curve obtained when using an illuminated pure TiO<sub>2</sub> wafer in the test solution. Significant bacterial inactivation was observed within ca. 5 minutes of photoirradiation, with the bacterial cell count detection limit reached within ca. 30 minutes. When an SPH wafer (two samples in duplicate) was photoirradiated in the test solution, the bacterial cell count detection limit was also reached within 30 minutes (Fig. 3), but with some differences (that will be discussed later on). Thus, the solar disinfection rate in the presence of the TiO<sub>2</sub> or SPH wafers is more than 10 times faster than with no photocatalyst present (Fig. 1–3).

It is important to note that the differences in the time taken for a significant reduction in the *E. coli* population occur because different disinfection mechanisms occur in the presence or absence of a photocatalyst. In the SODIS technique, bacterial inactivation results from direct exposure to UVA light

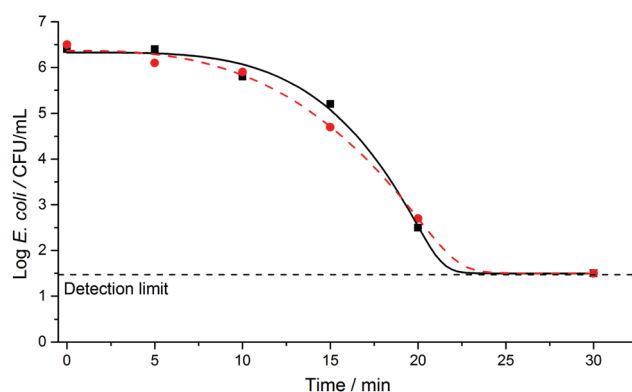


**Fig. 3** *E. coli* inactivation over a 30-minute period under irradiation from a 75 W xenon lamp in the presence of a TiO<sub>2</sub>-WO<sub>3</sub> heterojunction ceramic wafer. The filled square (■) and circle (●) are for two different experiments on identical samples and using the same protocols. The solid and dashed lines show data fits using the Weibull with tail model.



and heat, resulting in cellular membrane damage and a decreased rate of bacterial growth.<sup>38</sup> Formation of ROS can also occur when photons are absorbed by dissolved oxygen in the water, and these species may also contribute to the SODIS effect. In the presence of a photocatalyst, however, the main disinfection mechanism is believed to arise from cellular attack by ROS species.<sup>16</sup> It is suggested that the hydroxyl radical (OH<sup>•</sup>) is primarily responsible for inactivation of microorganisms,<sup>23</sup> while there are also reports that other ROS species, such as superoxide radicals (O<sub>2</sub><sup>•-</sup>), can affect survivability of microorganisms.

Comparison between the *E. coli* disinfection with the TiO<sub>2</sub> and TiO<sub>2</sub>-WO<sub>3</sub> heterojunction wafers shows a clear difference in the kinetics of the two systems (Fig. 2 and 3). For the pure TiO<sub>2</sub> wafer there is an initial, fast reduction in the microbial population, followed by a gradual decrease in the rate of inactivation. In contrast for the SPH wafer, the initial bacterial reduction rate is slower, but this is then followed by a clear increase in the rate of inactivation. The differences apparent between these two photoactive semiconducting systems can be explained in terms of electron-hole transfer lifetimes. The electron-hole recombination rate is expected to be substantially greater in the pure TiO<sub>2</sub> than the SPH wafer, because the latter incorporates a heterojunction that facilitates efficient vectorial charge separation, and allows build-up (longer lifetimes) of these charges, which can facilitate the production of ROS for bacterial inactivation.

The authors have previously shown that for photoirradiation of the titania side of TiO<sub>2</sub>-WO<sub>3</sub> SPH wafers, electrons can rapidly shuttle to the WO<sub>3</sub> side.<sup>27</sup> Once at the WO<sub>3</sub> surface, these electrons can reduce the W<sup>6+</sup> and also O<sub>2</sub> molecules to form O<sub>2</sub><sup>•-</sup> or H<sub>2</sub>O<sub>2</sub>, which then undergo reductive decomposition to form OH<sup>•</sup> radicals.<sup>39</sup> The holes at the TiO<sub>2</sub> surface can also oxidise species such as surface-adsorbed H<sub>2</sub>O to form OH<sup>•</sup> radicals with disinfective properties.<sup>9</sup>

The immobilisation of photocatalysts in solar water disinfection is of importance, particularly in locations where post-filtration may not be available. Previously, Alrousan *et al.* studied the solar disinfection of water under flow, using TiO<sub>2</sub> immobilised on the internal surface of borosilicate glass tubes. Microorganism inactivation occurred over a period of 5 hours, with no delamination of the TiO<sub>2</sub> coating occurring.<sup>23</sup> While immobilisation of a photocatalyst on a substrate proved effective, the self-supported nature of the pressed wafers presented herein removes the need for a thin-film substrate, along with associated production costs. Additionally, scale-up of

pressed wafers such as those described can be readily achieved by using industrial powder processing techniques to manufacture larger quantities of such self-supported photocatalyst structures, as larger planar area devices suitable for high throughput disinfection processes.

### Evaluation of disinfection kinetics

Since the first reports of photocatalytic water disinfection by Matsunaga *et al.*,<sup>40</sup> most kinetic data have been modelled using the Chick-Watson model,<sup>5</sup> which is applicable to the log-linear bacterial inactivation phase of the curve. While this region is of most interest, it is also important to model the kinetics occurring in other regions of the bacterial inactivation cycle in order to understand the complete disinfection process. In this work, the GInaFIT model<sup>30</sup> was used to quantitatively compare the kinetics of bacterial disinfection for experiments conducted under simulated solar irradiation, in the presence or absence of a photocatalyst. The GInaFIT model provides a total of nine potential models that can be applied to bacterial inactivation kinetic data. The suitability of each model can be determined by comparing the root mean square error (RMSE) values obtained for each. Table 1 provides the RMSE values for the various models used in this work that are in the range 0.10–0.23. Because it was necessary to allow the bacterial solution to homogenise after each measurement, it was not possible to reduce the sampling interval to less than 5 minutes, and this limited the number of data points that could be obtained to constrain kinetic models.

The curve presented for bacterial inactivation under photoirradiation only (Fig. 1) begins with an initial lag period followed by a bacterial inactivation phase. The initial lag phase is often termed a “shoulder” on the kinetic data and there are many suggestions relating to its existence. Geeraerd *et al.* stated that the shoulder phase exists because (i) if the bacteria exist in a clump, then all bacteria cells in that clump must be inactivated in order to completely inactivate that particular colony, and (ii) if the cells are able to synthesise a critical component, then inactivation only occurs when the rate of destruction is greater than the rate of synthesis.<sup>32</sup> Berney *et al.*<sup>41</sup> and Marugán *et al.*<sup>42</sup> state that there exists both a multi-hit scenario in which a single target must be hit multiple times for complete inactivation, and a multi-target scenario in which a single organism contains multiple targets that must each be hit for complete inactivation.

**Table 1** Kinetic parameters obtained from the GInaFIT tool with the log-linear with shoulder, Weibull, and Weibull with tail models

Sample	Shoulder length, $S_1$	Rate constant, $k_{\max}$	Scale parameter, $\delta$	Shape parameter, $p$ (min)	Root mean square error, RMSE
Simulated SODIS	2.9 ± 0.1 hours	4.70 ± 0.11 h <sup>-1</sup>	—	—	0.1375
TiO <sub>2</sub>	—	—	0.01 ± 0.01	0.20 ± 0.10	0.1015
TiO <sub>2</sub> -WO <sub>3</sub> (1)	—	—	14.15 ± 0.97	3.89 ± 0.73	0.2262
TiO <sub>2</sub> -WO <sub>3</sub> (2)	—	—	12.51 ± 0.88	2.79 ± 0.39	0.1708



The GInaFIT tool allowed quantification and comparison of the model output curves by providing various parameters depending on the fitting model chosen. For the log-linear with shoulder model, the parameters provided were the shoulder length,  $S_1$ , and the first order rate constant,  $k_{\max}$ . The shoulder length was the lag time before the log-linear bacterial inactivation began; for the simulated SODIS experiment shown herein (Fig. 1), this is  $2.9 \pm 0.1$  hours (Table 1). The first order rate constant for this experiment was  $4.7 \pm 0.1 \text{ h}^{-1}$ .

For the *E. coli* inactivation conducted in the presence of a pure  $\text{TiO}_2$  wafer or a  $\text{TiO}_2\text{-WO}_3$  SPH wafer, the Weibull, and Weibull with tail models, respectively, were determined as providing the best fits to the data. In these models, different parameters were defined: a scale parameter  $\delta$  and a shape parameter  $p$ .  $\delta$  was denoted as the time taken to achieve the first decimal reduction in bacterial population, and  $p$  related to the curvature of the fit; for  $p > 1$ , convex curves are obtained, and for  $p < 1$ , concave curves are observed. For these types of curves, first-order kinetics correspond to  $p = 1$ . The disinfection curves for the  $\text{TiO}_2$  (Fig. 2) and  $\text{TiO}_2\text{-WO}_3$  (Fig. 3) wafers showed different curvatures; the former fitted well with a concave curve, while the latter fitted with a convex curve. The respective  $p$  values (Table 1) correlated well with these observations. For the two types of wafers, however, the detection limit was reached within *ca.* 30 minutes in both cases. Comparing both scenarios, it should be noted that the disinfection kinetics for the  $\text{TiO}_2\text{-WO}_3$  SPH wafer would be beneficial to the overall disinfection rate since efficient vectorial electron-hole separation across the heterojunction would sustain the continuous formation of ROS species. This characteristic would be particularly attractive for treating bacterial strains that are typically more resistant to disinfection processes.

## Conclusions

The findings presented herein demonstrate that mechanically robust ceramic semiconducting hetero junction wafers, prepared by a simple and low-cost method, are suitable for efficient use in solar disinfection processes. The self-supported nature of the ceramic wafers removes the need for a thin-film substrate, which simplifies their preparation and removes much of the associated cost. Once the disinfection process is completed, the wafers can be easily removed from solution. In comparison to a pure  $\text{TiO}_2$  wafer, the two layer  $\text{TiO}_2\text{-WO}_3$  SPH wafer promotes efficient and sustained electron-hole separation. Although the initial solar disinfection rate appeared slower for the SPH than for the pure  $\text{TiO}_2$  wafer, the overall rate may be more sustainable due to efficient charge separation across the heterojunction.

To our knowledge, this is the first demonstration of such pressed ceramic wafers in solar disinfection applications. There is considerable potential to exploit such simple devices, using different combinations of photocatalysts, in other disinfection applications such as flow processes where there may be a number of infective agents present. The results of these endeavours will be reported in due course.

## Acknowledgements

EPSRC and UCL are thanked for provision of a studentship (N.M.M). The authors gratefully acknowledge Professor J. Byrne and Dr P. Dunlop for initial discussions relating to the experimental procedures carried out in this work. Professor Ivan P. Parkin and Professor Andrew Mills are thanked for discussions relating to the heterojunction wafers.

## Notes and references

- 1 U. Nations, Millennium Development Goals Report 2012, June 2012, ISBN 978-92-1-101258-3, available at: <http://mdgs.un.org/unsd/mdg/Resources/Static/Products/Progress2012/English2012.pdf>, accessed on 27/05/2014.
- 2 K. G. McGuigan, R. M. Conroy, H.-J. Mosler, M. du Preez, E. Ubomba-Jaswa and P. Fernandez-Ibañez, Solar water disinfection (SODIS): A review from bench-top to roof-top, *J. Hazard. Mater.*, 2012, **235–236**, 29–46.
- 3 E. Ubomba-Jaswa, M. A. R. Boyle and K. G. McGuigan, Inactivation of enteropathogenic *E. coli* by solar disinfection (SODIS) under simulated sunlight conditions, *J. Phys.: Conf. Ser.*, 2008, **101**, 012003.
- 4 E. Ubomba-Jaswa, C. Navntoft, M. I. Polo-Lopez, P. Fernandez-Ibanez and K. G. McGuigan, Solar disinfection of drinking water (SODIS): an investigation of the effect of UV-A dose on inactivation efficiency, *Photochem. Photobiol. Sci.*, 2009, **8**, 587–595.
- 5 M. N. Chong, B. Jin, C. W. Chow and C. Saint, Recent developments in photocatalytic water treatment technology: a review, *Water Res.*, 2010, **44**, 2997–3027.
- 6 J. Cao, B. Xu, H. Lin and S. Chen, Highly improved visible light photocatalytic activity of  $\text{BiPO}_4$  through fabricating a novel p-n heterojunction  $\text{BiOI/BiPO}_4$  nanocomposite, *Chem. Eng. J.*, 2013, **228**, 482–488.
- 7 C. W. Dunnill, S. Noimark and I. P. Parkin, Silver loaded  $\text{WO}_{3-x}/\text{TiO}_2$  composite multifunctional thin films, *Thin Solid Films*, 2012, **520**, 5516–5520.
- 8 H. Huang, S. Wang, N. Tian and Y. Zhang, A one-step hydrothermal preparation strategy for layered  $\text{BiIO}_4/\text{Bi}_2\text{WO}_6$  heterojunctions with enhanced visible light photocatalytic activities, *RSC Adv.*, 2014, **4**, 5561.
- 9 R. Quesada Cabrera, E. R. Latimer, A. Kafizas, C. S. Blackman, C. J. Carmalt and I. P. Parkin, Photocatalytic activity of needle-like  $\text{TiO}_2/\text{WO}_{3-x}$  thin films prepared by chemical vapour deposition, *J. Photochem. Photobiol., A*, 2012, **239**, 60–64.
- 10 D. O. Scanlon, C. W. Dunnill, J. Buckeridge, S. A. Shevlin, A. J. Logsdail, S. M. Woodley, C. R. A. Catlow, M. J. Powell, R. G. Palgrave, I. P. Parkin, G. W. Watson, T. W. Keal, P. Sherwood, A. Walsh and A. A. Sokol, Band alignment of rutile and anatase  $\text{TiO}_2$ , *Nat. Mater.*, 2013, **12**, 798–801.
- 11 F. Wang, X. Chen, X. Hu, K. S. Wong and J. C. Yu,  $\text{WO}_3/\text{TiO}_2$  microstructures for enhanced photocatalytic oxidation, *Sep. Purif. Technol.*, 2012, **91**, 67–72.



- 12 H. Wang, L. Zhang, Z. Chen, J. Hu, S. Li, Z. Wang, J. Liu and X. Wang, Semiconductor heterojunction photocatalysts: design, construction, and photocatalytic performances, *Chem. Soc. Rev.*, 2014, **43**, 5234–5244.
- 13 Y. Wang, Q. Wang, X. Zhan, F. Wang, M. Safdar and J. He, Visible light driven type II heterostructures and their enhanced photocatalysis properties: a review, *Nanoscale*, 2013, **5**, 8326.
- 14 Y. P. Yuan, L. W. Ruan, J. Barber, S. C. J. Loo and C. Xue, Hetero-nanostructured suspended photocatalysts for solar-to-fuel conversion, *Energy Environ. Sci.*, 2014, **7**, 3934–3951.
- 15 S. Malato, P. Fernández-Ibáñez, M. I. Maldonado, J. Blanco and W. Gernjak, Decontamination and disinfection of water by solar photocatalysis: Recent overview and trends, *Catal. Today*, 2009, **147**, 1–59.
- 16 J. A. Byrne, P. A. Fernandez-Ibañez, P. S. M. Dunlop, D. M. A. Alrousan and J. W. J. Hamilton, Photocatalytic Enhancement for Solar Disinfection of Water: A Review, *Int. J. Photoenergy*, 2011, **2011**, 1–12.
- 17 P. Dunlop, J. A. Byrne, N. Manga and B. R. Eggins, The photocatalytic removal of bacterial pollutants from drinking water, *J. Photochem. Photobiol., A*, 2002, **148**, 355–363.
- 18 P. Fernández, J. Blanco, C. Sichel and S. Malato, Water disinfection by solar photocatalysis using compound parabolic collectors, *Catal. Today*, 2005, **101**, 345–352.
- 19 C. Sichel, J. Tello, M. de Cara and P. Fernández-Ibáñez, Effect of UV solar intensity and dose on the photocatalytic disinfection of bacteria and fungi, *Catal. Today*, 2007, **129**, 152–160.
- 20 C. Sichel, J. Blanco, S. Malato and P. Fernández-Ibáñez, Effects of experimental conditions on *E. coli* survival during solar photocatalytic water disinfection, *J. Photochem. Photobiol., A*, 2007, **189**, 239–246.
- 21 P. S. M. Dunlop, T. A. McMurray, J. W. J. Hamilton and J. A. Byrne, Photocatalytic inactivation of *Clostridium perfringens* spores on TiO<sub>2</sub> electrodes, *J. Photochem. Photobiol., A*, 2008, **196**, 113–119.
- 22 D. M. Alrousan, P. S. Dunlop, T. A. McMurray and J. A. Byrne, Photocatalytic inactivation of *E. coli* in surface water using immobilised nanoparticle TiO<sub>2</sub> films, *Water Res.*, 2009, **43**, 47–54.
- 23 D. Alrousan, M. I. Polo-López, P. Dunlop, P. Fernández-Ibáñez and J. A. Byrne, Solar photocatalytic disinfection of water with immobilised titanium dioxide in re-circulating flow CPC reactors, *Appl. Catal., B*, 2012, **128**, 126–134.
- 24 C. Pablos, R. van Grieken, J. Marugán, I. Chowdhury and S. L. Walker, Study of bacterial adhesion onto immobilized TiO<sub>2</sub>: Effect on the photocatalytic activity for disinfection applications, *Catal. Today*, 2013, **209**, 140–146.
- 25 O. Akhavan, M. Abdollahad, Y. Abdi and S. Mohajezadeh, Synthesis of titania/carbon nanotube heterojunction arrays for photoinactivation of *E. coli* in visible light irradiation, *Carbon*, 2009, **47**, 3280–3287.
- 26 S. Elouali, A. Mills, I. P. Parkin, E. Bailey, P. F. McMillan and J. A. Darr, Photocatalytic evolution of hydrogen and oxygen from ceramic wafers of commercial titanias, *J. Photochem. Photobiol., A*, 2010, **216**, 110–114.
- 27 N. M. Makwana, R. Quesada-Cabrera, I. P. Parkin, P. F. McMillan, A. Mills and J. A. Darr, A simple and low-cost method for the preparation of self-supported TiO<sub>2</sub>-WO<sub>3</sub> ceramic heterojunction wafers, *J. Mater. Chem. A*, 2014, **2**, 17602–17608.
- 28 A. Mills and J. Wang, Simultaneous monitoring of the destruction of stearic acid and generation of carbon dioxide by self-cleaning semiconductor photocatalytic films, *J. Photochem. Photobiol., A*, 2006, **182**, 181–186.
- 29 E. S. Patera and J. R. Holloway, A non-end-loaded piston-cylinder device for use up to 40 kbar, *Eos, Trans., Am. Geophys. Union*, 1978, **59**, 1217–1218.
- 30 A. H. Geeraerd, V. P. Valdramidis and J. F. Van Impe, GInaFiT, a freeware tool to assess non-log-linear microbial survivor curves, *Int. J. Food Microbiol.*, 2005, **102**, 95–105.
- 31 D. A. Ratkowsky, in *Modeling Microbial Responses in Foods*, ed. R. McKellar and X. Lu, CRC Press, Boca Raton, 2003, pp. 151–196.
- 32 A. H. Geeraerd, C. H. Herremans and J. F. Van Impe, Structural model requirements to describe microbial inactivation during a mild heat treatment, *Int. J. Food Microbiol.*, 2000, **59**, 185–209.
- 33 I. Albert and P. Mafart, A modified Weibull model for bacterial inactivation, *Int. J. Food Microbiol.*, 2005, **100**, 197–211.
- 34 J. Lonnen, S. Kilvington, S. C. Kehoe, F. Al-Touati and K. G. McGuigan, Solar and photocatalytic disinfection of protozoan, fungal and bacterial microbes in drinking water, *Water Res.*, 2005, **39**, 877–883.
- 35 M. Berney, H. U. Weilenmann, A. Simonetti and T. Egli, Efficacy of solar disinfection of *Escherichia coli*, *Shigella flexneri*, *Salmonella Typhimurium* and *Vibrio cholerae*, *J. Appl. Microbiol.*, 2006, **101**, 828–836.
- 36 M. Boyle, C. Sichel, P. Fernández-Ibáñez, G. B. Arias-Quiroz, M. Iriarte-Puna, A. Mercado, E. Ubomba-Jaswa and K. G. McGuigan, Bactericidal Effect of Solar Water Disinfection under Real Sunlight Conditions, *Appl. Environ. Microbiol.*, 2008, **74**, 2997–3001.
- 37 M. Agulló-Barceló, M. I. Polo-López, F. Lucena, J. Jofre and P. Fernández-Ibáñez, Solar Advanced Oxidation Processes as disinfection tertiary treatments for real wastewater: Implications for water reclamation, *Appl. Catal., B*, 2013, **136–137**, 341–350.
- 38 A. Hamamoto, M. Mori, A. Takahashi, M. Nakano, N. Wakikawa, M. Akutagawa, T. Ikehara, Y. Nakaya and Y. Kinouchi, New water disinfection system using UVA light-emitting diodes, *J. Appl. Microbiol.*, 2007, **103**, 2291–2298.
- 39 J. Kim, C. W. Lee and W. Choi, Platinized WO<sub>3</sub> as an Environmental Photocatalyst that Generates OH Radicals under Visible Light, *Environ. Sci. Technol.*, 2010, **44**, 6849–6854.
- 40 T. Matsunaga, R. Tomoda, T. Nakajima and H. Wake, Photoelectrochemical sterilization of microbial cells by



- semiconductor powders, *FEMS Microbiol. Lett.*, 1985, **29**, 211–214.
- 41 M. Berney, H. U. Weilenmann, J. Ihssen, C. Bassin and T. Egli, Specific Growth Rate Determines the Sensitivity of *Escherichia coli* to Thermal, UVA, and Solar Disinfection, *Appl. Environ. Microbiol.*, 2006, **72**, 2586–2593.
- 42 J. Marugán, R. van Grieken, C. Sordo and C. Cruz, Kinetics of the photocatalytic disinfection of *Escherichia coli* suspensions, *Appl. Catal., B*, 2008, **82**, 27–36.

